Nuclear Instruments and Methods in Physics Research A 698 (2013) 177–184

Contents lists available at SciVerse ScienceDirect

Nuclear Instruments and Methods in Physics Research A

journal homepage: www.elsevier.com/locate/nima

Improvements in the Monte Carlo code for simulating 4πβ(PC)–γ coincidence system measurements

M.S. Dias [a,*], M.N. Takeda [b], F. Toledo [a], F. Brancaccio [a], M.L.O. Tongu [a], M.F. Koskinas [a]

[a] Instituto de Pesquisas Energéticas e Nucleares, IPEN-CNEN/SP, Av. Prof. Lineu Prestes 2242, 05508-000 São Paulo, SP, Brazil
[b] Universidade Santo Amaro, UNISA Rua Prof. Enéas da Siqueira Neto 340, 04829-300 São Paulo, SP, Brazil

ARTICLE INFO

Article history:
Received 18 June 2012
Received in revised form
4 October 2012
Accepted 4 October 2012
Available online 12 October 2012

Keywords:
Monte Carlo
Standardization
Coincidence
Radionuclide

ABSTRACT

A Monte Carlo simulation code known as ESQUEMA has been developed by the Nuclear Metrology Laboratory (Laboratório de Metrologia Nuclear—LMN) in the Nuclear and Energy Research Institute (Instituto de Pesquisas Energéticas e Nucleares—IPEN) to be used as a benchmark for radionuclide standardization. The early version of this code simulated only β−γ and ec−γ emitters with reasonably high electron and X-ray energies. To extend the code to include other radionuclides and enable the code to be applied to software coincidence counting systems, several improvements have been made and are presented in this work.

1. Introduction

The Monte Carlo simulation code ESQUEMA [1,2] developed by the Nuclear Metrology Laboratory (Laboratório de Metrologia Nuclear–LMN) in the Nuclear and Energy Research Institute (Instituto de Pesquisas Energéticas e Nucleares–IPEN) can be used as a benchmark for radionuclide standardization by calculating the expected extrapolation curve and considering the parameters of the radionuclide decay chain and the detailed characteristics of the detection system. In this code, the detector response functions are calculated using a radiation transport Monte Carlo code. The results are used to solve the coincidence equations, allowing simulation of an entire experiment from the detection mechanism to the output spectra and activity results. A modified version of this code was applied to a 4πβ(PS)−γ coincidence system [3], which uses plastic scintillators in a 4π geometry, and the corresponding response functions were calculated using the PENELOPE software package [4].

The early version of ESQUEMA [1,2] applied to 4πβ(PC)−γ systems considered only β−γ and ec−γ emitters with reasonably high electron and X-Ray energies (tens of keV), and the response functions were calculated using MCNP-4C [5]. Despite this limitation, the code was able to successfully simulate several radionuclides [1,2,6,7]. To update the transport code to utilize MCNPX [8] and to extend ESQUEMA to include other radionuclides, several improvements were implemented and are discussed in the present work.

This code was devised for general application, but the present work is focused on the following radionuclides: ^{22}Na, ^{99m}Tc, ^{177}Lu, ^{198}Au, ^{123}I and ^{152}Eu, which were experimentally standardized using the LMN and compared against the Monte Carlo simulations. With the exception of ^{152}Eu, experimental results for these radionuclides have already been published in the literature [9–13], and thus, only a brief review is given here. In the case of ^{152}Eu, detailed discussions on the measurements and results are provided in the present paper.

2. Methodology

2.1. Coincidence equations

A full description of the coincidence equations can be found elsewhere [e.g., [14–16]]. The general formulae applied to the coincidence measurements are given by:

$$\frac{N_\beta N_\gamma}{N_c} = N_0 \times \left\{ \frac{\sum_{i=1}^{m} a_i \left\{ \varepsilon_{\beta_i} + (1-\varepsilon_{\beta i}) \sum_{j=1}^{n} b_{ij} \frac{\alpha_{ij}[\varepsilon_{ce_{ij}} + (1-\varepsilon_{ce_{ij}})\varepsilon_{(X,A)ij}] + \varepsilon_{\beta\gamma_{ij}}}{1+\alpha_{ij}} \right\} \sum_{i=1}^{m} a_i \sum_{j=1}^{n} b_{ij} \varepsilon_{\gamma_{ij}} \frac{1}{1+\alpha_{ij}}}{\sum_{i}^{m} a_i \left[\varepsilon_{\beta_i} \sum_{j=1}^{n} b_{ij} \varepsilon_{\gamma_{ij}} \frac{1}{1+\alpha_{ij}} + (1-\varepsilon_{\beta_i}) \sum_{j=1}^{n} b_{ij} \varepsilon_{c_{ij}} \frac{1}{1+\alpha_{ij}} \right]} \right\} \quad (1)$$

where N_β, N_γ and N_c are the beta, gamma and coincidence counting rates, respectively; N_0 is the disintegration rate; a_i and

* Correspondence to: Instituto de Pesquisas Energéticas e Nucleares, IPEN-CNEN/SP, Centro do Reator de Pesquisas-CRPq, C.P. 11049, Pinheiros, 05422-970 São Paulo, SP, Brazil. Tel.: +55 11 3133 8779; fax: +55 11 3133 9960.
E-mail address: msdias@ipen.br (M.S. Dias).

0168-9002/$ - see front matter © 2012 Elsevier B.V. All rights reserved.
http://dx.doi.org/10.1016/j.nima.2012.10.018

b_{ij} are the intensity per decay of the i-th beta transition and the relative intensity of the j-th transition with respect to the i-th transition; n is the number of daughter transitions following the i-th beta transition; m is the number of beta transitions; $\varepsilon_{\beta i}$ is the beta efficiency associated with the i-th beta transition; $\varepsilon_{\gamma ij}$, and $\varepsilon_{\beta\gamma ij}$ are the gamma detection efficiency and the gamma efficiency of the beta detector, respectively, associated with the ij-th transition; ε_{ceij} and $\varepsilon_{(X,A)ij}$ are the conversion electron detection efficiency and the Auger electron or X-ray detection efficiency, respectively, associated with the ij-th transition, and ε_{ceij} and α_{ij} are the gamma-gamma coincidence detection efficiency and the total internal conversion coefficient of the ij-th transition.

An estimate of the beta efficiency may be derived using:

$$\frac{N_c}{N_\gamma}=\frac{\sum_i^m a_i\left[\varepsilon_{\beta_i}\sum_{j=1}^n b_j\varepsilon_{\gamma_{ij}}1/1+\alpha_{ij}+(1-\varepsilon_{\beta_i})\sum_{j=1}^n b_j\varepsilon_{C_{ij}}1/1+\alpha_{ij}\right]}{\sum_{i=1}^m a_i\sum_{j=1}^n b_{ij}\varepsilon_{\gamma_{ij}}1/1+\alpha_{ij}} \quad (2)$$

The extrapolation curve is obtained by plotting $N_\beta N_\gamma/N_c$ vs. $(1-N_c/N_\gamma)/N_c/N_\gamma$, and the disintegration rate N_0 is obtained in the limit in which the beta efficiency parameter goes to one: $N_c/N_\gamma\to 1$ implies $N_\beta N_\gamma/N_c\to N_0$. The term $(1-N_c/N_\gamma)/(N_c/N_\gamma)$ is usually called the *inefficiency parameter*. For radionuclides that decay through electron capture, the symbol β should be changed to ec in the above equations.

The purpose of the Monte Carlo code ESQUEMA is to provide a theoretical plot of $N_\beta N_\gamma/N_c$ vs. $(1-N_c/N_\gamma)/(N_c/N_\gamma)$ to simulate the extrapolation curve. To achieve this goal, all details of the decay scheme and the detection system must be considered. The use of this code is important because the experimental efficiency of a 4π(PC) detector is never one and may be quite low in some cases, for example, for radionuclides that decay through electron capture. Therefore, a reliable curve must be accurately extrapolated from the maximum experimental efficiency to 100% to obtain the activity of the radioactive source.

Some radionuclides decay through a mixture of processes, such as β^-, β^+ and electron capture, with different branching probabilities. When only two branches are considered, for instance, β^- and electron capture, high-order terms may be neglected, and a simplified coincidence equation may be used:

$$\frac{N_{4\pi}}{\varepsilon_\beta\varepsilon_{ec}}=N_0\left[1+a_1\frac{(1-\varepsilon_\beta)}{\varepsilon_\beta}+a_2\frac{(1-\varepsilon_{ec})}{\varepsilon_{ec}}\right] \quad (3)$$

Or alternatively,

$$\frac{N_{4\pi}}{\varepsilon_\beta\varepsilon_{ec}}=N_0\left\{a_1'\left[1+\frac{(1-\varepsilon_{ec})}{\varepsilon_{ec}}\right]+a_2'\left[\frac{(1-\varepsilon_\beta)}{\varepsilon_\beta}-\frac{(1-\varepsilon_{ec})}{\varepsilon_{ec}}\right]\right\} \quad (4)$$

where $N_{4\pi}$ is the total counting rate of the 4π(PC) detector; ε_β is the efficiency parameter for the beta branch $(N_c/N_\gamma)_\beta$; ε_{ec} is the efficiency parameter for the electron capture branch $(N_c/N_\gamma)_{ec}$; N_0 is the radioactive source activity; a_1, a_2, a_1' and a_2' are fitting parameters.

Eq. (4) provides the value of the electron capture decay branch probability from the ratio a_1'/a_2'.

To properly simulate Eqs. (3) and (4), the Monte Carlo simulation must include two sets of decay branches as input parameters: one for the β^- transition and another for the electron capture transition. This configuration is equivalent to simulating two radionuclides in a single run and was applied to the ^{152}Eu calibration.

The final activity value is obtained using a Least Square fitting procedure that considers the following Chi-Squared value:

$$\chi^2=\left(\vec{y}_{\exp}-N_0\vec{y}_{MC}\right)^T V^{-1}\left(\vec{y}_{\exp}-N_0\vec{y}_{MC}\right) \quad (5)$$

where $\vec{y}_{\exp}$ is the experimental vector of $N_\beta N_\gamma/N_c$; $\vec{y}_{MC}$ is the $N_\beta N_\gamma/N_c$ vector calculated from the Monte Carlo with unit activity; N_0 is the activity of the radioactive source; V is the total covariance matrix, including both experimental and calculated uncertainties; and T represents the matrix transposition.

A series of simulated values are calculated using a wide range of beta efficiency parameters and small efficiency intervals. The theoretical value to be used in Eq. (1) is obtained using linear interpolation to the corresponding experimental efficiency.

In the case of mixed-decay radionuclides, the experimental and simulated vectors, $\vec{y}_{\exp}$ and $\vec{y}_{MC}$, should be substituted with the left term given by Eq. (3), and the corresponding pair of experimental efficiencies, ε_β and ε_{ec}, must match the simulated pair.

2.2. Experimental setup

Two coincidence systems, called I and II, were used in the experiments. These systems are composed of a 4π gas-flow proportional counter (PC) coupled to one or two NaI(Tl) crystals. In System I, a thin aluminum window is provided to allow the NaI(Tl) detector to perform X-ray measurements. Alternatively, this system can be operated at high pressures, up to 1.0 MPa, and coupled to an HPGe spectrometer for high resolution gamma-ray measurements if necessary. In System II, a pair of 50.8 mm × 76.2 mm NaI(Tl) scintillators are coupled in a sandwich geometry, and a 3.0 mm thick wall at the PC counter allows only high energy (> 100 keV) photons to be detected by the scintillators.

The standardizations described in the present work span several years, and the LMN electronic setup has undergone several improvements over this period. The standardization of ^{22}Na was performed using an old electronic system consisting of standard coincidence and timer/counter NIM modules [17]. The electronic system used in the ^{177}Lu, ^{198}Au and ^{123}I standardizations was improved by replacing some of the electronic modules with a Time to Amplitude Converter (TAC) [17,18], and the activity was calculated using the CONTAC [19] software developed at the LMN.

A Software Coincidence System (SCS) was used for the standardizations of ^{99m}Tc and ^{152}Eu. This system is based on the National Instruments PCI-6132 card, capable of up to four independent analog inputs, and the signals were processed using the NI LabVIEW 2010 Platform acquisition program [20–22]. Information about the pulse height and time of occurrence were registered for both the beta and gamma channels along with a third channel corresponding to a reference pulser to check deadtime corrections. The activity was calculated using a software coincidence code called SCTAC [23], also developed at the LMN.

2.3. Radionuclides to be simulated by the Monte Carlo code

Certain improvements made to the Monte Carlo code, related to detection system geometry and photon detection in the PC counter, may affect the radionuclide simulations; these improvements are described in Sections 2.4.1 and 2.4.2, respectively. A few special radionuclides standardized by the LMN required specific additional improvements. The decay characteristics of these radionuclides and their special requirements are detailed in Sections 2.3.1–2.3.3. The corresponding necessary improvements to the Monte Carlo simulations are described in Sections 2.4.3–2.4.6.

2.3.1. ^{22}Na

This radionuclide decays by β^+ emission in 90.3% of decays and by electron capture in 9.64%, mostly to the 1274 keV excited state of ^{22}Na [24]. The experimental procedure developed by the

LMN for this standardization was part of an international comparison with PTB mediated by the BIPM [25], and the measurements were performed using both Systems I and II. In System I, the HPGe detector was replaced by a 50.8 mm × 76.2 mm NaI(Tl) scintillator. The PC efficiency was altered due to the addition of external absorbers above and below the radioactive sources. Two gamma windows were used for the calibration: the first at the 1274 keV total absorption peak and the second at the (511+1274) keV summed peak. A more detailed description of the experimental procedure developed by the LMN for this standardization is provided elsewhere [9,25].

The first improvement necessary to simulate these experiments was the addition of a positron response function for the PC counter. An additional effect had to be considered in the calibration that selected the gamma-ray window at the 511 keV annihilation peak or at the summed peak: the variation of the annihilation photon detection efficiency due to variations in the positron position inside the PC counter. The conventional response functions for the NaI(Tl) scintillators had to be changed to account for this effect.

2.3.2. ^{99m}Tc

This radionuclide decays primarily to ^{99}Tc with very weak β^- emission [26]; therefore, conventional $\beta-\gamma$ or $ec-\gamma$ coincidence techniques are not suited to detecting the decay. However, System I provides a thin window in the PC counter that allows X-ray measurements by the NaI(Tl) scintillator. This feature enables the use of coincidence between conversion electrons measured at the PC counter and the K X-rays following this process, measured at NaI(Tl) scintillator. The experimental procedure developed by LMN to standardize this radionuclide is described in detail elsewhere [10].

The previous version of ESQUEMA did not consider coincidences between conversion electrons and X-rays. An extension to lower energies had to be incorporated in the NaI(Tl) photon response functions, and MCNPX input geometry was finely tuned to describe the strong attenuation of low-energy photons in the detection system materials. A new loop in the code was added to calculate the necessary parameters, spectra and extrapolation curves for this radionuclide.

Changing the PC efficiency by adding absorbers above and below the radioactive sources is difficult for this radionuclide due to its short half-life. Instead, implementing pulse height discrimination in the software coincidence system, described in Section 2.2, turned out to be much more convenient. To utilize this procedure, the experimental and simulated PC spectra must be in good agreement. Therefore, resolution effects in the PC counter had to be included in the simulation.

2.3.3. ^{152}Eu

The experimental standardization of ^{152}Eu using the $4\pi\beta(PC)-\gamma$ coincidence method is described in the present work. This radionuclide decays by electron capture in 72.1% of decays, β^+ emission to ^{152}Sm in 0.027% of decays and β^- emission to ^{152}Gd in 27.9% of decays [27]. Neglecting the β^+ contribution, there are two main branches to consider: electron capture and β^-emission. In addition, this nuclide undergoes a multitude of gamma transitions. Therefore, it was necessary to use an HPGe detector and to build up a photon response function for this detector by applying the MCNPX code with a narrow energy bin (1 keV).

Because both decay branches contribute to the HPGe gamma-ray spectra, the Monte Carlo simulation must include two input decay data tables, one for each branch. The final gamma-ray spectrum is a mixture of all gamma-rays that appear in the decay scheme, considering each individual intensity and detection efficiency.

The activity is obtained using a double extrapolation curve, considering the inefficiency parameter for each decay branch, given by Eqs. (3) and (4), and selecting two gamma-ray windows: one for the electron capture branch and another for the β^- branch. The Monte Carlo simulation should be capable of predicting this bi-parametric extrapolation curve for comparison with experiment.

2.4. Improvements in the Monte Carlo simulation

2.4.1. Detection system geometry

In the early version of ESQUEMA [1,2], a simplified geometry that included only the 4π gas-flow proportional counter and a single NaI(Tl) scintillator was used in the MCNP calculations. At that time, MCNP-4C was used [5]. In the new version, all components surrounding the detectors were included, and the detailed geometry and materials of both systems were considered, including the radioactive source substrate.

The new models developed for Systems I and II are shown in Figs. 1 and 2, respectively. These drawings were produced using the VISED software included in the MCNP5 package [8]. In Fig. 1, a NaI(Tl) scintillator is positioned above the 4π detector, and an HPGe spectrometer is placed below. In Fig. 2, a pair of NaI(Tl) detectors are positioned above and below the 4π(PC) detector in a sandwich geometry. The detailed radioactive source holder configuration is presented in the zoomed figure at upper right. Region A is the radioactive source substrate, Region B is the 20 μg cm^{-2} Collodion film substrate coated with a 10 μg cm^{-2} gold layer in which the aliquot of radioactive material is deposited, and Region C is the 0.1 mm thick stainless steel holder. The surrounding circle in both figures corresponds to the escape sphere in the Monte Carlo calculation.

The detector position was checked by placing standard gamma-ray sources inside the 4π(PC) detector and comparing the experimental peak efficiency with the MCNPX predictions at several gamma energies for both the NaI(Tl) scintillators and HPGe spectrometer.

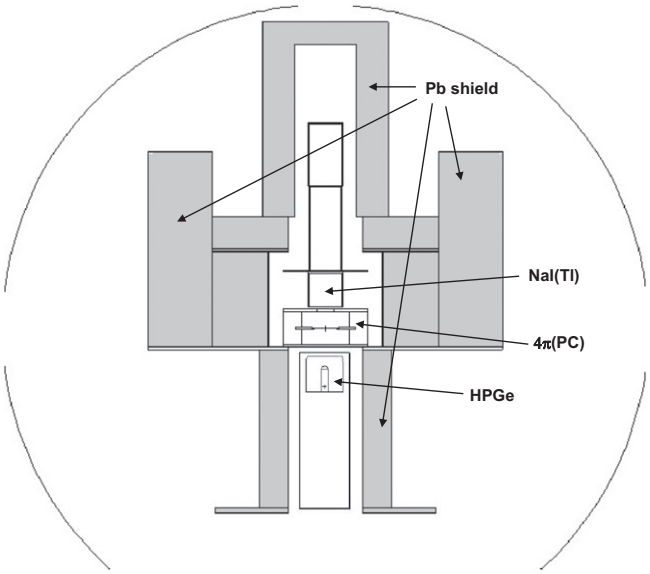

Fig. 1. Schematic diagram of the LMN Coincidence system I for radionuclide standardization. The NaI(Tl) scintillator is positioned above the 4π detector and the HPGe spectrometer is placed below. Lead shield is the gray region. The surrounding circle corresponds to the escape sphere in Monte Carlo calculation.

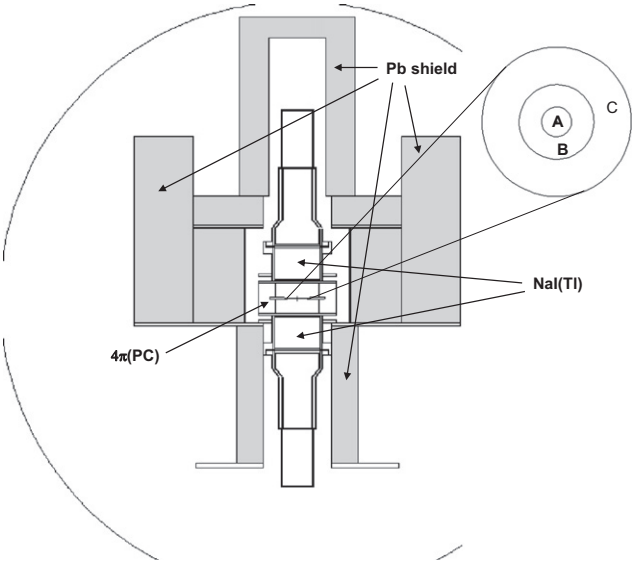

Fig. 2. Schematic diagram of the LMN Coincidence system II for radionuclide standardization. The pair of NaI(Tl) detectors are positioned above and below the 4π detector. Lead shield is the gray region. Detailed radioactive source holder configuration is zoomed in at upper right side. Region A is the radioactive source substrate; region B is the Collodion film and region C is the stainless steel holder. The surrounding circle corresponds to the escape sphere in Monte Carlo calculation.

The deposited energy spectra of both electrons and positrons in the 4π(PC) detector were calculated using MCNPX at 196 energies from 1.4 keV to 4000 keV. The number of histories followed was 5×10^4 at each energy. The spectra of energy deposited by photons in the HPGe detector were calculated for 3029 energies from 12 keV to 3035 keV in 1-keV bins. The same energy range was covered in 4 keV bins for photon detection with the pair of scintillators in System II. In both cases, 2×10^6 histories were followed at each photon energy.

2.4.2. Gamma-ray and X-ray detection in the proportional counter

A second improvement was the inclusion of gamma-ray and X-ray detection in the proportional counter. The gamma-ray detection efficiency corresponds to $\varepsilon_{\beta\gamma}$ in Eq. (1). X-ray detection is related to electron capture or conversion electron effects following radionuclide decay. Possible gamma-gamma coincidence between the PC counter and the scintillators was also considered by determining the fraction of energy deposited by the scattered gamma-ray in each detector.

The photon detection efficiency of a 4π gas-flow proportional counter is usually below 0.5% over a wide range of photon energies (20–2000 keV) but becomes large at very low (<10 keV) or very high photon energies (>3000 keV). This effect was considered by generating a new response table in MCNPX, which was included as input data to ESQUEMA. The differential energy spectra of photons in the 4π(PC) detector were calculated for 740 energies from 4 keV to 2992 keV in 4-keV bins. The number of histories followed was 2×10^6 at each energy.

Whenever beta or electron capture radiation (X-ray or Auger electron) is *not* detected in the PC counter and is *not* accompanied by a conversion electron, gamma-ray detection becomes possible and its contribution to N_β is calculated. An X-ray from electron capture decay can also be directly detected in the 4π(PC) detector. This effect has been added to Auger electron detection and was already incorporated in the early version. This effect is important for intermediate nuclei such as ^{54}Mn, for which the K X-ray energies are only a few keV and the detection efficiency may thus be high.

2.4.3. X-ray detection in the NaI(Tl) scintillator from conversion electron process

The use of a thin window in the PC detector in System I allows X-ray detection in the NaI(Tl) scintillator. Therefore, it becomes possible to measure coincidences between conversion electrons and X-rays. This effect is very important for certain radionuclides, e.g., ^{99m}Tc, for which the absence of beta emission and electron capture processes complicates the direct use of the coincidence formalism. For this purpose, the deposited energy spectra of photons in the NaI(Tl) detector of System I were calculated using MCNPX at 760 energies from 12 keV to 3048 keV in 4-keV bins.

2.4.4. Resolution effects in the 4π(PC) counter

A standard method of determining the radioactive source activity is to plot the extrapolation curve as discussed in Section 2.1. This curve is usually obtained by placing external absorbers above and below the radioactive source to change the efficiency of the 4π(PC) detector. In this method, low-energy electrons are absorbed first because of their smaller range. As more absorber is added, electrons of higher energies are gradually absorbed.

When a low-energy and a high-energy electron are mixed, the counts in the spectrum due to the low-energy electrons vanish as the absorber thickness increases, leaving only the counts due to the high-energy electrons. Low-energy electrons usually originate in beta emission or electron capture processes. On the other hand, conversion electrons usually have high energies and are not absorbed for a relatively wide range of absorber thicknesses; therefore, their detection efficiencies (ε_{ce}) remain near one. As a result, the slope of the extrapolation curve changes proportionally to $(1-\varepsilon_\beta)$, following the expected behavior predicted by Eq. (1). Although accurate, this procedure is cumbersome and very time-consuming because many experimental points are necessary to build a complete extrapolation curve.

An alternative method to change the efficiency of the 4π(PC) detector is to use pulse height discrimination. This method is very convenient when a software coincidence system is available, such as that recently installed at LMN [20]. In this case, all pulse amplitudes and the corresponding occurrence times for both the beta and gamma counting channels are recorded. With all of this information, it is possible to plot the complete extrapolation curve from a single measurement, saving a great deal of time while also keeping the radioactive source free from absorbers. However, the pulse height distribution of a gas-flow 4π proportional counter has a complex shape, and the pulse height discrimination method may not remove electrons of increasing energy as desired, due to the effects described below.

The 4π proportional counter installed at LMN is operated as a gas-flow counter and is not an electron spectrometer except at low electron energies (<50 keV) because the electron range at higher energies is larger than the electron path through the detector gas. Under these conditions, only a fraction of the initial electron energy is deposited in the gas, and the resulting pulse height is thus lower than expected. According to MCNPX calculations applied to the 4π detector geometry, the average energy deposited in the gas is approximately 10 keV for 100 keV electrons and approximately 4.4 keV for 1000 keV electrons, as shown in Fig. 3. This behavior can be explained by considering that the electron's specific energy losses due to ionization and excitation decrease as the electron energy increases [28]. Therefore, the resulting spectra for high-energy electrons are strongly distorted towards low pulse amplitudes. When two electron energies are mixed, e.g., one electron below 50 keV and another above

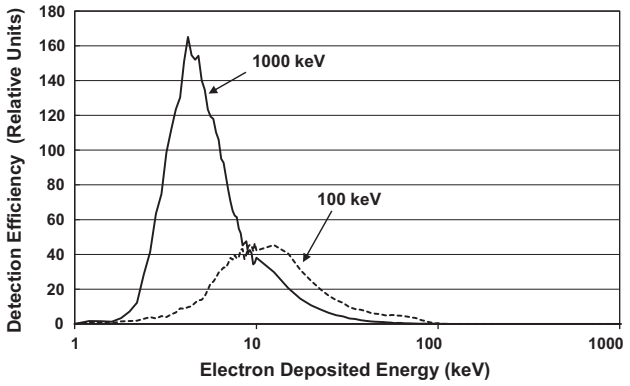

Fig. 3. Deposited electron energy spectra in the 4π proportional counter calculated by code MCNPX. The continuous curve corresponds to 1000 keV and the dashed curve corresponds to 100 keV initial electron energies, respectively.

100 keV, the pulses produced by electrons from these two energies will overlap. This effect can be predicted by MCNPX and has been included in the input response tables used by ESQUEMA to calculate the 4π(PC) pulse height spectrum.

The Poisson statistics of the number of ion pairs produced in the gas also affect the pulse height discrimination technique. The strength of this effect can be estimated by measuring the peak broadening at low electron energies. In the present work, a ^{99m}Tc source was measured to determine the resolution of K-Auger electrons at 15–18 keV. At other energies, this effect is determined using the usual $1/\sqrt{E_d}$ law, where E_d is the energy deposited in the gas, which is proportional to the pulse height.

To determine the extrapolation curve using pulse height discrimination, the 4π(PC) spectrum shape must be theoretically predicted. The inclusion of the effects described above in ESQUEMA enabled comparison of the calculated and experimental spectra, making the extrapolated activity accurately correspond to the correct source activity.

2.4.5. Positron annihilation inside the 4π(PC) counter

When studying pure β^+ or mixed β^+/EC emitters, it may be convenient to place the gamma-ray window at the 511 keV peak to detect β^+ and annihilation photon coincidence events. However, when applying this procedure, the gamma-ray efficiency changes with the absorber thickness because positron annihilation may occur at different positions inside of the 4π(PC) counter. Considering that constant gamma-ray efficiency is a necessary condition to obtain the correct extrapolation curve, this effect must be considered. Detailed consideration on this correction has already been described elsewhere [9].

2.4.6. Resolution effects in the HPGe spectrometer

For the HPGe spectrometer, the FWHM value corresponding to the full absorption energy peak follows an approximately linear relationship with the gamma ray energy. For this reason, a linear fit was applied to the experimental FWHM values and used to correct for the detector's finite resolution by broadening the gamma ray spectrum generated by ESQUEMA using a normal distribution with the experimentally determined FWHM.

2.4.7. Standardization of mixed decay radionuclides

Some radionuclides decay through a mixture of processes with different branch intensities. A typical example is ^{152}Eu, which has a complex decay scheme involving several transitions that populate the excited levels of ^{152}Sm and ^{152}Gd.

This radionuclide was calibrated by plotting a bi-parametric extrapolation curve that considered the 4π(PC) detector's efficiencies for both β^- and electron capture processes. For this purpose, two gamma-ray windows were set: one corresponding to a β^- transition at 344 keV and another one corresponding to an electron capture transition at 1408 keV. In this case, the β^+ transition can be neglected in activity standardization due to its very low intensity.

To properly simulate Eqs. (3) and (4), the Monte Carlo simulation of ^{152}Eu included two separate sets of decay branches as input parameters: one for β^- transitions and another for electron capture transitions. This configuration is equivalent to simulating two radionuclides in a single run.

3. Results and discussion

Fig. 4 shows the 4π gas-flow proportional counter photon efficiency calculated by MCNPX and the experimental results. At low photon energies, the efficiency is high, reaching 93% at 4 keV due to the high photoelectric absorption coefficient in the P-10 gas mixture. This coefficient decreases rapidly as the photon energy increases, reducing the counter efficiency to values near 0.1% at 300 keV. At energies above 500 keV, the efficiency starts to increase due to multiple photon interactions in the gas and detector walls.

In Fig. 4, the error bars in the calculation represent one standard deviation ($k=1$) and include the statistics of the MCNPX Monte Carlo calculation and the uncertainties in the PC gas density. Reasonable agreement is achieved between the Monte Carlo calculation and the experimental results obtained by Moura et al. [25] using ^{203}Hg, ^{51}Cr, ^{54}Mn, ^{60}Co and ^{88}Y radioactive sources. In the cases of ^{203}Hg and ^{51}Cr, the experimental values are near zero, and the error bars correspond to the one standard deviation ($k=1$) upper limit. Although the overall uncertainties are rather high (~20%), it must be emphasized that the parameter $\varepsilon_{\beta\gamma}$, which appears in the second term of Eq. (1), contributes very little to the activity value (< 0.1%), and the present results may therefore be considered satisfactory.

Fig. 5 shows the total absorption peak corresponding to K-X rays from ^{99m}Tc measured with the NaI(Tl) scintillator counter of System I (Fig. 1). This radionuclide decays by internal transition and has no beta or electron capture branches. Coincidence measurements were performed between the internal conversion electrons and the corresponding K-X rays [10]. Strong agreement is achieved between the Monte Carlo calculations and the

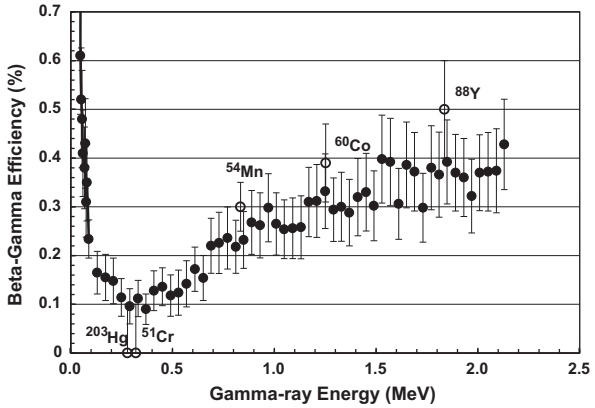

Fig. 4. Proportional counter efficiency to gamma-rays (in percent). The black marks correspond to Monte Carlo calculations by means of MCNPX, applying the geometrical models shown in Figs. 1 and 2. The white marks are experimental results taken from Moura et al. [25].

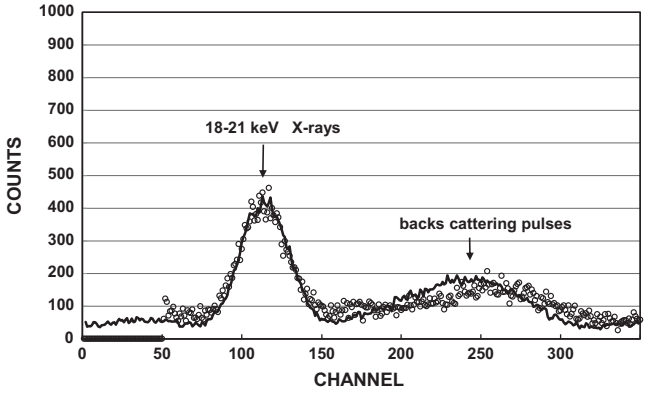

Fig. 5. Total absorption peak corresponding to 18–21 keV K-X rays from ^{99m}Tc, measured with NaI(Tl) scintillator counter in system I (Fig. 1). The continuous line corresponds to Monte Carlo calculations by means of code ESQUEMA and the white marks are experimental results obtained at the LMN [10].

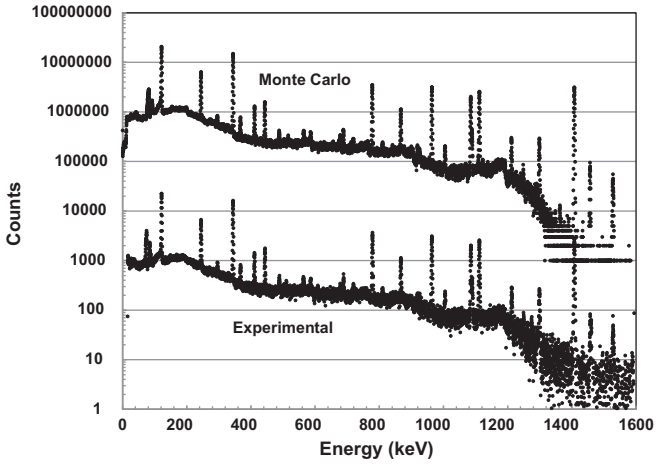

Fig. 6. Comparison between experimental HPGe ^{152}Eu spectrum (below) and Monte Carlo calculation by code ESQUEMA (above). The calculated spectrum has been multiplied by an arbitrary factor (10^3) to make it easier to compare with experiment.

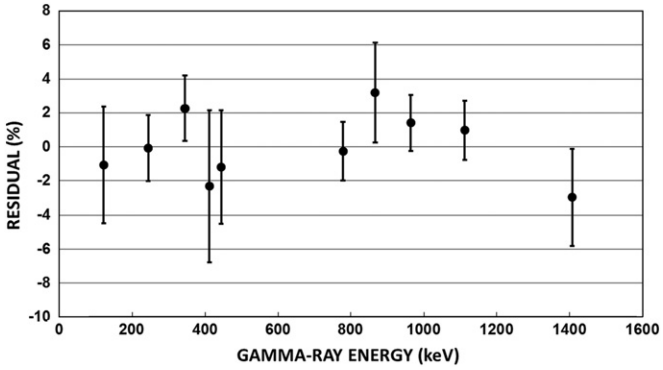

Fig. 7. Residuals between experimental total absorption peak net areas and those calculated by code ESQUEMA for HPGe ^{152}Eu gamma-ray spectra.

experimental results, primarily in the region of interest around the total energy absorption peak.

Fig. 6 shows the ^{152}Eu gamma-ray spectra obtained by the HPGe detector of System I. The lower points are the experimental results obtained at the LMN, and the upper points correspond to the Monte Carlo calculations of ESQUEMA. Strong qualitative agreement is evident. To quantitatively compare these results, the experimental and simulated net peak areas have been calculated for the primary gamma-ray transitions used for activity determination. The residuals between the experimental and calculated total absorption net peak areas are presented in Fig. 7 with the estimated overall uncertainties. No appreciable bias is observed, indicating that the MCNPX geometric model shown in Fig. 1 and the decay characteristics provided to ESQUEMA can be considered reliable. The uncertainty budget for this comparison is presented in Table 1. The net peak areas and their respective uncertainties were determined using the MAESTRO software package [29], and the cascade summing correction was calculated using Monte Carlo software developed at the LMN called COINCIG [30]. The uncertainty in the PC wall attenuation correction was estimated by assuming $a \pm 0.1$ mm uncertainty in the PC wall thickness and represents the dominant contribution to the overall uncertainty at low gamma-ray energies. The uncertainty in the MCNPX gamma-ray efficiency was estimated by comparing the calculated results with experimental measurements performed with a standard ^{152}Eu source supplied by the IAEA.

Because ^{152}Eu has a mixed decay scheme, this simulation is equivalent to simultaneously simulating two radionuclides. The intercept and slope (in keV) of the linear fit to the peak FWHM as a function of the gamma ray energy were 2.380 ± 0.023 and 0.000376 ± 0.00028, respectively. Fig. 8 presents the behavior of Eq. (3) calculated using Monte Carlo and compared to the experimental results from the coincidence measurements. In this calibration, the gamma-ray windows were set at the 344 keV total absorption peak for the β^- branch and at the 1408 keV total absorption peak for the electron capture branch. The calculated and experimental points appear indistinguishable in the figure because the difference between each pair ranged from -0.86% to $+1.98\%$. The extrapolated experimental source activity was (580.7 ± 4.3) kBq, and the value calculated using Eq. (3) was (579.0 ± 4.5) kBq, in excellent agreement. The uncertainty budget corresponding to this ^{152}Eu calibration is shown in Table 2. The primary contribution to the overall uncertainty arises from the bi-parametric fitting procedure. The gap between the extrapolated value and the first experimental (and calculated) data point arises because the maximum efficiency for electron capture events is low due to the low Auger electron emission probability and the proportional counter's low detection efficiency for X-rays from ^{152}Gd.

4. Conclusion

Several improvements have been implemented in ESQUEMA and are described in the present paper. The detailed geometry of the coincidence system was incorporated into the response function calculations, which were performed using MCNPX. Gamma and X-ray detection in the proportional counter and X-ray detection in the NaI(Tl), the annihilation quantum detection efficiency in the NaI(Tl) as a function of positron energy and the resolution functions of PC and HPGe detectors were added to the ESQUEMA code. All of these changes enabled the simulation of additional radionuclides that were experimentally calibrated using the $4\pi(PC)\beta-\gamma$ system at the LMN: ^{22}Na [16], ^{177}Lu [20], ^{198}Au [21], ^{123}I [22], ^{99m}Tc [19] and ^{152}Eu (present paper).

ESQUEMA was primarily intended to be applied to the LMN coincidence systems. However, other laboratories may be able to apply the same code to their own systems. The only requirement is the photon and electron response functions for each detector in the coincidence system, which can be determined using any

Table 1
Uncertainty budget for the ratios between experimental gamma-ray net peak areas and those calculated by code ESQUEMA for ^{152}Eu, in percent ($k=1$).

Source of uncertainty (%)	Gamma energy (keV)									
	121.78	244.69	344.27	411.11	443.96	778.90	867.38	964.07	1112.07	1408.01
Net area-experimental	0.32	0.83	0.30	2.35	1.76	0.76	1.90	0.72	0.69	0.51
Source attenuation-experimental	0.44	0.32	0.28	0.27	0.26	0.20	0.19	0.18	0.17	0.15
Cascade summing-experimental	0.40	0.43	0.26	0.56	0.63	0.35	0.49	0.19	0.04	0.11
Statistics-MCNPX	0.67	0.63	0.73	0.79	0.81	1.00	1.09	1.13	1.19	1.31
PC wall attenuation-MCNPX	3.18	1.19	0.90	0.80	0.77	0.57	0.54	0.52	0.48	0.43
Gamma-ray efficiency-MCNPX	0.57	0.29	1.38	2.70	1.81	0.47	0.36	0.19	0.41	2.35
Net area-ESQUEMA	0.34	0.79	0.31	2.30	1.68	0.68	1.68	0.62	0.73	0.49
Gamma intensity-ESQUEMA	0.46	0.53	0.41	0.45	0.45	0.46	0.59	0.41	0.44	0.43
Total (%)	3.42	1.94	1.94	4.47	3.33	1.72	2.95	1.65	1.75	2.85

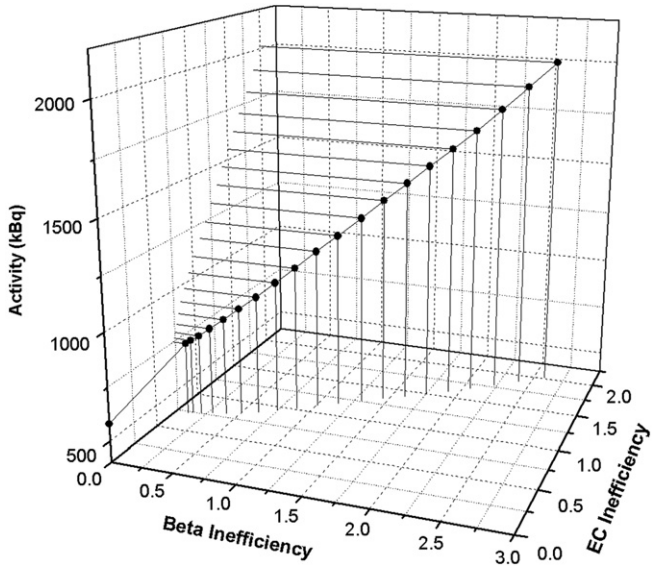

Fig. 8. Extrapolation curve between observed activity and inefficiency parameters for ^{152}Eu, according to Eq. (3). The calculated and experimental points are indistinguishable in the figure because they are less than 2% apart. The gap between the first and second points is due to electron capture maximum experimental efficiency which is far from unity (~58%).

Table 2
Uncertainty budget for the ^{152}Eu activity obtained experimentally and by means of Eq. (3), in percent ($k=1$).

Source of uncertainty	Value ($k=1$) (%)
Decay correction	0.15
Radioactive source mass	0.20
Efficiency parameter	0.11
Statistics-beta counting	0.01
Fitting procedure-experimental	0.69
Fitting procedure-Monte Carlo	0.73
Total experimental	0.74
Total Monte Carlo	0.78

radiation transport code such as MCNPX [8] or PENELOPE [4]. Consideration of the surrounding objects is important because they can produce X-rays or scattering photons that may affect the detector response functions. The decay scheme information is read from an additional file that can be built easily from data available in the literature. The files corresponding to radionuclides already standardized by the LMN can be supplied to interested members of the community.

Acknowledgments

The authors are indebted to the National Council for Scientific and Technological Development (CNPq) from Brazil for partial support of the present research.

References

[1] M.N. Takeda, M.S. Dias, M.F. Koskinas, IEEE Transactions on Nuclear Science NS-52 (5) (2005) 1716.
[2] M.S. Dias, M.N. Takeda, M.F. Koskinas, Applied Radiation and Isotopes 64 (2006) 1186.
[3] M.S. Dias, H. Piuvezam-Filho, A.M. Baccarelli, M.N. Takeda, M.F. Koskinas, Nuclear Instruments and Methods in Physics Research A 580 (2007) 380.
[4] F. Salvat, J.M. Fernandez-Varea, E. Costa, J. Sempau, PENELOPE-2001: Code System to Perform Monte Carlo Simulation of Electron Gamma-Ray Showers in Arbitrary Materials, RSICC CODE PACKAGE CCC-682, RSICC Computer Code Collection, 2001.
[5] O.R.N.L., Monte Carlo N-Particle Transport Code System, MCNP-4C, RSICC Computer Code Collection, Oak Ridge National Laboratory, Report CCC-700, 2001.
[6] N.L. Maidana, M.N. Takeda, M.S. Dias, M.F. Koskinas, V.R. Vanin, Nuclear Instruments and Methods in Physics Research A 553 (2005) 559.
[7] M.F. Koskinas, E.A. Silva, I.M. Yamazaki, M.S. Dias, Applied Radiation and Isotopes 66 (2008) 934.
[8] ORNL, Monte Carlo N-Particle Transport Code System, MCNP5, RSICC Computer Code Collection, Oak Ridge National Laboratory, 2006.
[9] M.S. Dias, M.L.O. Tongu, M.N. Takeda, M.F. Koskinas, Applied Radiation and Isotopes 68 (2010) 1362.
[10] B. Brito, M.F. Koskinas, F. Litvak, F. Toledo, M.S. Dias, Applied Radiation and Isotopes 70 (2012) 2097.
[11] M.S. Dias, F.F.V. Silva, M.F. Koskinas, Applied Radiation and Isotopes 68 (2010) 1349.
[12] D.S. Moreira, M.F. Koskinas, M.S. Dias, I.M. Yamazaki, Applied Radiation and Isotopes 68 (2010) 1566.
[13] M.F. Koskinas, K.C. Gishitomi, A.B. Brito, I.M. Yamazaki, M.S. Dias, Applied Radiation and Isotopes 70 (2012) 2091.
[14] P.J. Campion, International Journal of Applied Radiation and Isotopes 4 (1959) 232.
[15] A. Gandy, International Journal of Applied Radiation and Isotopes 11 (1961) 75.
[16] A.P. Baerg, Nuclear Instruments and Methods 112 (1973) 143.
[17] W.O. Lavras, M.F. Koskinas, M.S. Dias K.A. Fonseca, Primary standardization of ^{51}Cr radioactive solution. in: Proceedings of the V Regional Congress on Radiation Protection and Safety IRPA, in CDROM, 2001.
[18] M. Baccarelli, M.S. Dias, M.F. Koskinas, Applied Radiation and Isotopes 58 (2003) 239.
[19] M.S. Dias, CONTAC: A Code for Activity Calculation Based on TAC Measurements. Internal Report, IPEN-CNEN/SP, 2001.
[20] F. Toledo, F. Brancaccio, M.S. Dias, Design of electronic system with simultaneous registering of pulse amplitude and event time applied to the $4\pi\beta-\gamma$ coincidence method, International Nuclear Atlantic Conference-INAC, in CDROM Santos, SP, Brazil, September 30 to October 5, 2007.
[21] National Instruments, 〈http://www.ni.com/〉 (accessed June 2012).
[22] National Instruments, 〈http://www.ni.com/labview/pt/〉 (accessed June 2012).
[23] M.S. Dias, SCTAC: A Code for Activity Calculation based on Software Coincidence Counting Measurements. Internal Report, IPEN-CNEN/SP, 2010.
[24] M. Galan, CIEMAT, Recommended Data, 〈http://www.nucleide.org/DDEP_WG/DDEPdata.htm〉, ^{22}Na Table, 2009.

[25] L.P. Moura, A.B..Nuevo-Jr., IEA Report on the Standardization of ^{22}Na, Mediated by the BIPM (in connection with the PTB), 1973.
[26] C. Morillon, M.M. Bé, V. Chechev, A. Egorov, Table of Radionuclides 1 (2004) 183.
[27] V.R. Vanin, R.M. de Castro, E. Browne, Table of Radionuclides 2 (2004) 1.
[28] G.F. Knoll, Radiation Detection and Measurement, 4th edition, John Wiley & Sons, Inc., 2010.
[29] ORTEC, Advanced Measurement Technology, MAESTRO for Windows, Version 6.01, 2003, 〈http://www.ortec-online.com/Solutions/applications-software.aspx〉.
[30] M.S. Dias, M.N. Takeda, M.F. Koskinas, Applied Radiation and Isotopes 56 (2002) 105.